JTTEE5 19:368–377
DOI: 10.1007/s11666-009-9433-z
1059-9630/$19.00 © ASM International

Behavior of HVOF WC-10Co4Cr Coatings with Different Carbide Size in Fine and Coarse Particle Abrasion

Arash Ghabchi, Tommi Varis, Erja Turunen, Tomi Suhonen, Xuwen Liu, and S.-P. Hannula

(Submitted April 24, 2009; in revised form October 12, 2009)

A modified ASTM G 65 rubber wheel test was employed in wet and dry conditions using 220 nm titania particles and 368 μm sand particles, respectively. Both tests were conducted on WC-CoCr coatings produced with two powders with different carbide grain sizes (conventional and sub-micron) to address the effect of carbide size and abrasive medium characteristics on the wear performance. The same spot before and after the wet abrasion wear testing was analyzed in detail using SEM to visualize wear mechanisms. It was shown that the wear mechanism depends on the relative size of the carbide and abrasive particles. Wear mechanisms in dry sand abrasion were studied by analyzing the single scratches formed by individual abrasive particles. Interaction of surface open porosity with moving abrasive particles causes formation of single scratches. By tailoring the carbide size, the wear performance can be improved.

Keywords HVOF, rubber wheel abrasion test, WC-CoCr, wear mechanism

1. Introduction

Ceramic-metallic (cermet) materials in the form of thermally sprayed coatings have been employed successfully on different industrial components where good wear performance is needed (Ref 1). This class of materials offers a combination of hardness and toughness. Reinforcement particles in the form of carbides or oxides are responsible for hardness, whereas the binder matrix is responsible for toughness in cermet materials. Among the cermet coatings deposited by thermal spray techniques, WC-Co has gained great interest due to its good resistance against wear (Ref 2). It has been shown that addition of chromium to the cobalt binder improves the corrosion resistance of WC-Co (Ref 3). Accordingly, good corrosion resistance alongside good wear performance makes WC-CoCr coating an admirable candidate for applications where both corrosion and wear resistance are critical.

There are different test methods for evaluation of wear performance of a coating system. In each particular method, testing variables have diverse and significant effects on the evaluation of wear performance and the associated wear mechanisms. It is important to choose proper test methods and test parameters to mimic real working conditions. By simulating the actual wear condition in different applications, laboratory-based results will be more useful and reliable. One of the important testing variables in abrasion is abrasive particle size. In some applications, such as paper and pulp industries, there are nano-sized abrasive particles varying in shape which exist in the medium and can be softer or harder than the coating material. Most of the investigations for abrasive wear study of thermal spray coatings have been done by employing abrasive particles on the order of tens of microns which are significantly larger than reinforced hard particles and binder mean free path of coatings (Ref 4-6). Changes in wear performance as well as wear mechanisms by changing the abrasive particle size from micro to nano are expected.

One of the most crucial parameters that effects mechanical properties and wear performance of carbide-based cermet coatings is carbide grain size. For carbide-based cermets, researchers have shown a gain in wear performance by reducing the carbide size (Ref 7). The driving force for reducing the carbide grain size comes from the fact that as the carbide size becomes smaller, the binder mean free path is decreased, resulting in higher resistance against deformation and material loss. Many researchers (Ref 4, 8-17) have pursued such a hypothesis

This article is an invited paper selected from presentations at the 2009 International Thermal Spray Conference and has been expanded from the original presentation. It is simultaneously published in *Expanding Thermal Spray Performance to New Markets and Applications: Proceedings of the 2009 International Thermal Spray Conference*, Las Vegas, Nevada, USA, May 4-7, 2009, Basil R. Marple, Margaret M. Hyland, Yuk-Chiu Lau, Chang-Jiu Li, Rogerio S. Lima, and Ghislain Montavon, Ed., ASM International, Materials Park, OH, 2009.

Arash Ghabchi, Tommi Varis, Erja Turunen, and **Tomi Suhonen,** Technical Research Center of Finland (VTT), Espoo, Finland; **Xuwen Liu** and **S.-P. Hannula**, Department of Materials Science and Engineering, Helsinki University of Technology, Espoo, Finland; and **Arash Ghabchi**, Department of Material Science and Engineering, Center for Thermal Spray Research, SUNY Stony Brook. Contact e-mail: arash.ghabchi@vtt.fi.

to improve the wear performance of HVOF WC-Co by reducing the WC grain size to the nanoscale. Nevertheless, for thermal spray coatings, different researchers have shown sometimes contradictory wear performance results for the effect of reducing carbide size from conventional to nano (Ref 5, 18).

In this work, we studied the possible advantages in mechanical properties and wear performance by reducing WC grain size in WC-CoCr coating deposited by HVOF technique. Wear loss was measured quantitatively as mass or volume loss. Some of the mechanical properties were evaluated as well. The wear mechanisms of coating which showed best wear resistance were studied in detail.

2. Experimental Techniques

2.1 Materials

Two different WC-CoCr powders with different WC grain size were used in this study: conventional (WOKA 3652, Sulzer Metco, Germany) and sub-micron (DURMAT 135.063, Durum, Germany). Detailed characteristics of the powders are provided in Table 1.

2.2 Coating Deposition

All coatings were deposited by HVOF DJ-Hybrid gun using the hydrogen as the fuel gas and nitrogen as the carrier gas. The parameter selection was based on temperature and velocity measurements made by a Spraywatch diagnostic device (Oseir Oy, Finland). Two sets of spray parameters were selected for deposition of coatings. These parameters are shown in Table 2. The temperature and velocity are shown in Fig. 1 for both powders and spraying parameters. It is notable that parameter "A" provides higher temperature with lower velocity, while parameter "B" provides lower temperature with higher velocity. Coatings were deposited on stainless steel that was grit-blasted with 590-710 μm alumina particles at 4.5 bar pressure followed by ultrasonic cleaning in the acetone. Enough air cooling was applied to keep the substrate temperature at 150 °C during spraying. Substrate temperature was measured during the spraying to assure the minimal fluctuation from intended substrate temperature (±50 °C).

Table 1 Details of employed powders in this study

Powders	Apparent density, g/cm^3	WC grain size, μm	Size distribution d10-d90%	Chemical composition, wt.%		
				C	Co	Cr
Conventional	4.91	1-3	24-45	5.34	9.68	3.79
Sub-micron	5.71	0.4	20-39	5.13	9.98	4.0

Table 2 Spraying parameters

Parameters	H_2, SLM	O_2, SLM	N_2, SLM	Air, SLM	Fuel/ oxygen	Stand-off distance, mm
A	635	215	14	350	2.2	230
B	605	245	20	350	1.9	230

SLM, standard liters per minute

2.3 Characterization Techniques

Coatings were evaluated by x-ray diffraction with a Phillips PW3710 with Mo-K-α radiation for detection of different phases and the W_2C/WC intensity peak ratio was used as an indication of the level of decarburization. Powders and coatings cross sections were studied by scanning electron microscopy (SEM), JEOL JSM-6400. The shape of abrasive particles utilized in this work was studied by SEM. Hardness and elastic modulus values were obtained by an instrumented microhardness tester (Zwick ZHU 0.2). A Vickers indenter was employed using a 300 g load for hardness and elastic modulus measurement. Wear performance was evaluated by volume loss in a wet abrasion test using a Sensofar surface profilometry instrument and by weight loss in a dry sand abrasion test. Porosity values were measured using five SEM images of coating cross sections with 500× magnification by LeicaQwin image analyzing software.

2.4 Abrasive Wear Test

There are different apparatus for abrasion test based on ASTM standards such as ASTM G65 and B611 (Ref 19, 20) specifically designed for cemented carbides. We used two different modified abrasion test techniques to carry out both dry and wet abrasion tests. Figure 2 shows two modified settings used in this study. In both cases, a rubber wheel was used to provide low stress level in dry and wet conditions.

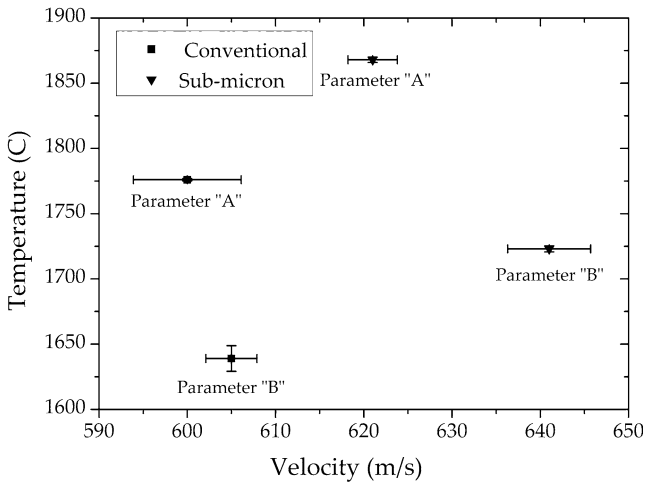

Fig. 1 Temperature and velocity measured for spraying parameters "A" and "B" for conventional and sub-micron powders

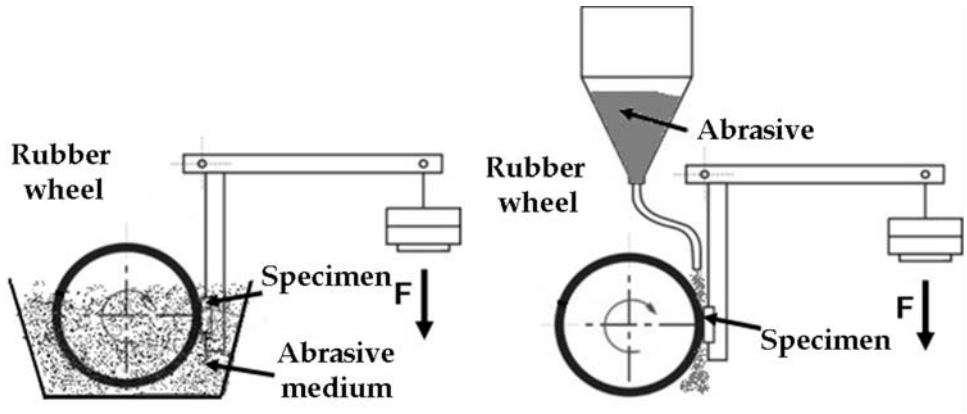

Fig. 2 Modified settings used in this study for wet (left) and dry (right) rubber wheel abrasion wear test

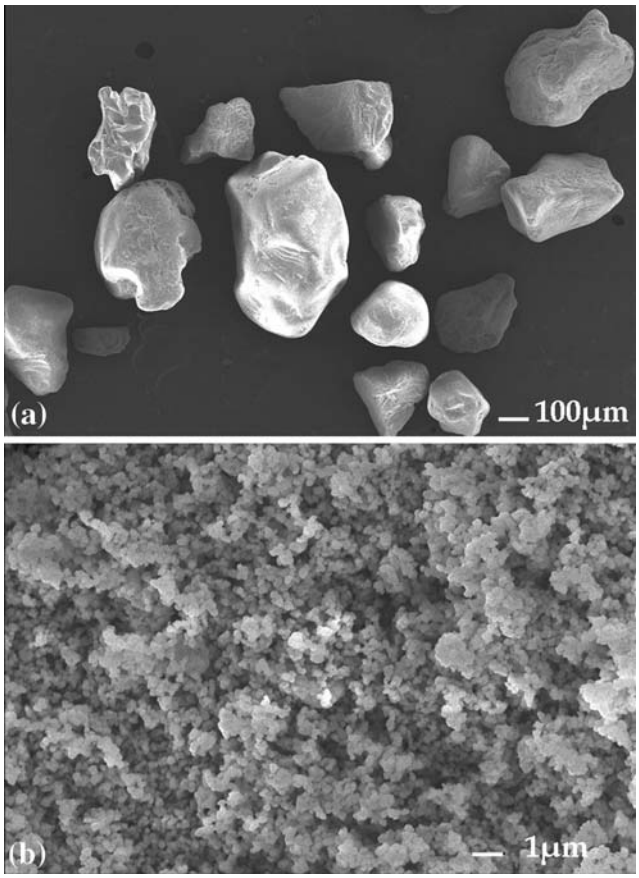

Fig. 3 (a) Sand abrasive particles with irregular shape used in dry abrasion test and (b) titania abrasive particles with spherical shape used in wet abrasion test

The abrasive particles that were used in the dry rubber wheel tests were casting sand particles (99.5% SiO_2) with a 368 μm diameter. Figure 3(a) shows the SEM image of sand abrasive particles. It is notable that sand abrasives contain both irregular- and spherical-shape particles. No recycling of abrasive particles was done during the dry rubber wheel abrasion test. Mass loss of samples was measured at different time intervals (10, 20, and 30 min) as an indication for wear performance during dry rubber wheel abrasion testing. Wheel speed was 200 rpm and feeding rate of sand particles was 260 g/min. Both tests were done under 5 kg load.

For wet abrasion testing, a mixture of 10% mass titania in water was used. Average particle size of employed titania was 220 nm. Size distribution of titania particles in the water mixture was measured to make sure no permanent bonding of particles has happened in the mixture. Hardness of titania and casting sand particles are relatively the same (750-950 HV). A wheel speed of 100 rpm was used for wet abrasion test. The volume loss of coating was measured after 6-h tests as an indication of wear performance. Figure 3(b) shows the SEM picture of titania abrasive particles. As depicted, the titania particles are uniformly spherical.

3. Results and Discussion

3.1 Coating Characterization and Wear

Figure 4 shows the backscattered electron images of conventional and sub-micron powder morphology and cross sections used in this study. In the case of conventional powder, the binder phase is not completely homogenized. Nevertheless, for sub-micron powder, the binder is completely homogenized. The difference in level of homogeneity is arising from differences in the powder manufacturing processes. It is shown from the cross-sectional images that conventional powder has lower density. The SEM figures from the coating microstructures are presented in Fig. 5, which shows clearly the difference in carbide size and binder mean free path between the coatings. In Table 3, W_2C/WC ratio, indentation hardness, indentation elastic modulus, porosity, and wear performance of coatings for different spray conditions are presented. The level of decarburization (W_2C/WC ratio) for coatings deposited using sub-micron powder is higher than conventional and for the coatings sprayed by conventional

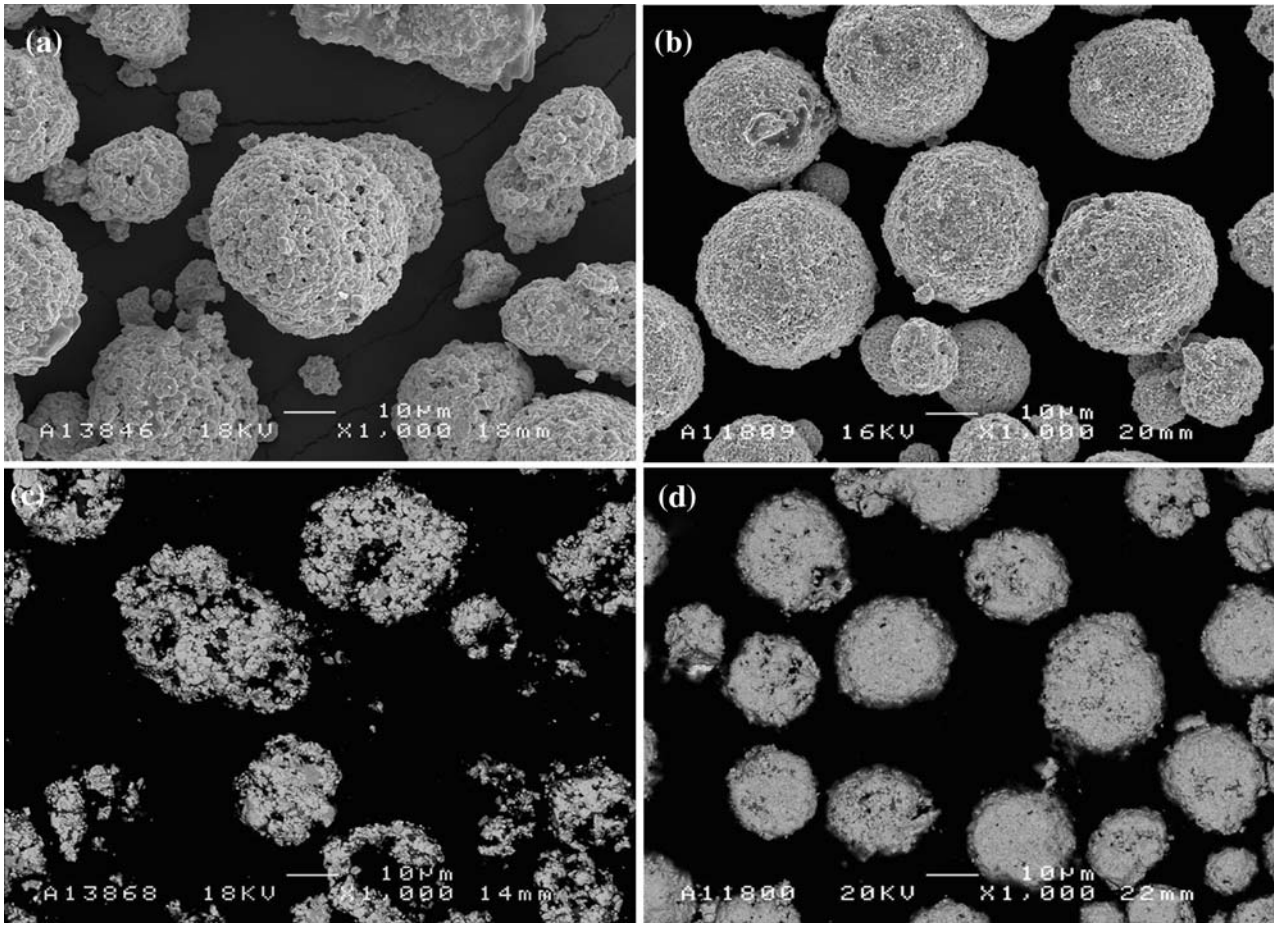

Fig. 4 Conventional powder morphology (a) and cross section (c). Sub-micron powder morphology (b) and cross section (d)

carbide size powder, the difference in W_2C content is relatively low and changing the spraying parameters has no significant effect on W_2C content. Nevertheless, W_2C content in finer carbide size is more sensitive to spraying parameters. This might be attributed to higher tendency of finer WC to dissolute into the matrix (Ref 21).

3.2 Wear Mechanism in Fine Particle Wet Abrasion

The volume losses after 6 h of wet abrasion testing are presented in Fig. 6. It can be seen that wear performance in fine particle wet abrasion for sub-micron coatings, disregarding to the spraying parameters, is better.

The coating, which was deposited by conventional powder using parameter ''B'', exhibits the worst wear performance under both dry and wet abrasion. This might be due to the lower heat input that led to the poor microstructure with a high amount of porosity. Among the coatings deposited by sub-micron powder, the coating sprayed with parameter ''B'', which had the lowest porosity, exhibited the best wear performance in wet abrasion.

To systematically study the wear mechanism, a visualization approach was employed by means of studying the same spot on the wet abrasion wear track with low and high resolutions. Patterned indents using a Vickers indenter were made with a 10 kg load on the surface of sample to serve as landmarks for relocating purpose. Using this marking technique, we were able to relocate the same spot in the electron microscope. This technique enables us to relocate individual carbides with high resolution in the microstructure by interrupting the abrasion test and examining the sample using SEM. This technique allowed for studying the wear mechanism on different scales. Figure 7 shows a schematic of this procedure. After marking the sample, the SEM images were taken before the wet abrasion test, after 3 h of testing and after 6 h of testing exactly from the same spot. The SEM images taken from the targeted spot before the test did not reveal any features of microstructure due to poor surface quality (not presented here). Because of the sample size, we were not able to apply polishing on the samples and only lapping was applied prior to wet abrasion wear test.

In the microscale range (Fig. 8), it was observed that some of the pores became bigger and some others became smaller (shown by arrows in Fig. 8a, b). We hypothesize this is due to non-uniform material removal from the

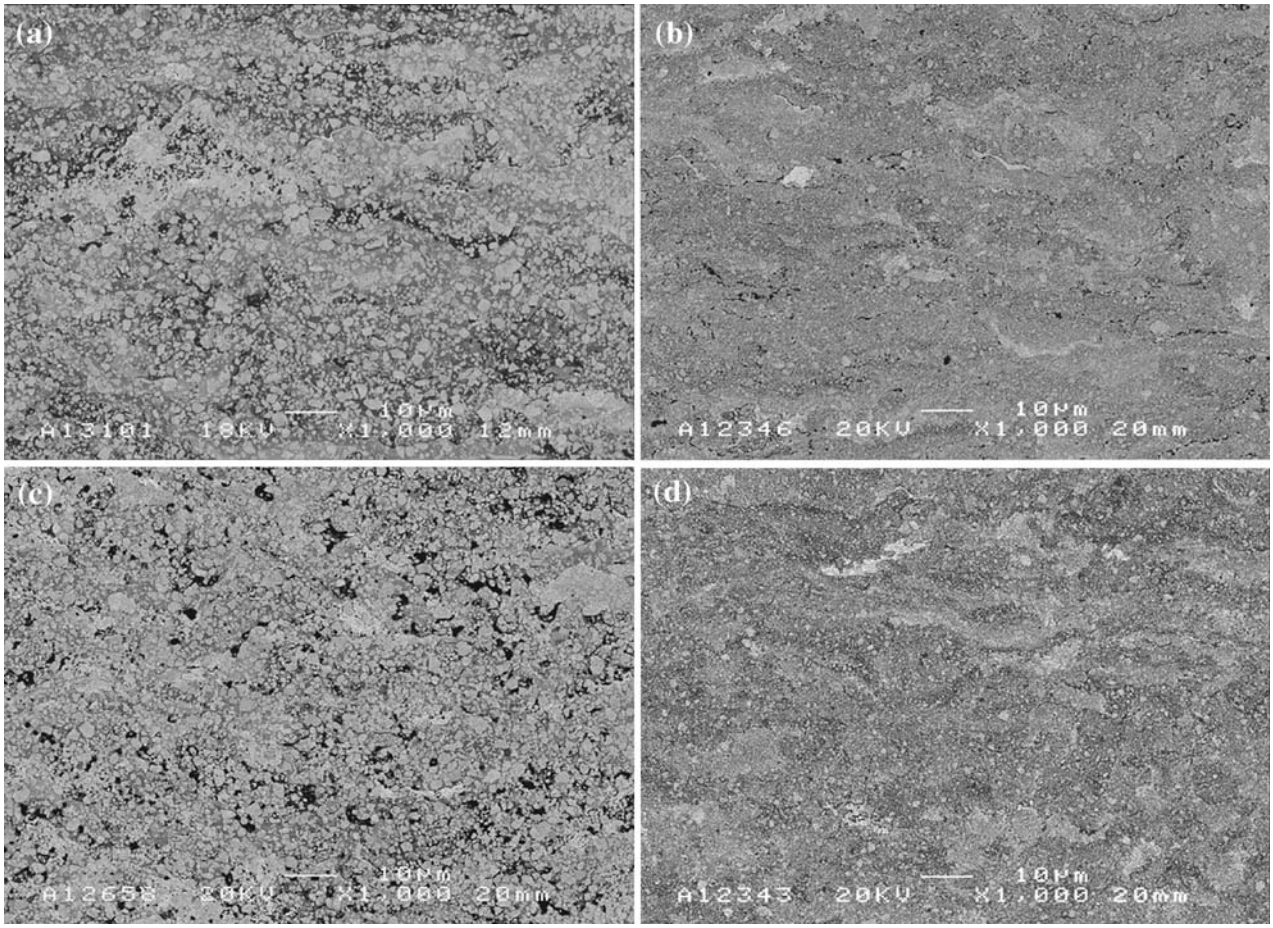

Fig. 5 SEM microstructures from the coating sprayed by conventional powder with parameters A (a) and B (c) and sub-micron powder sprayed with parameters A (b) and B (d)

Table 3 Coatings properties

Powder	Parameter	W_2C/WC	Hardness, HV 0.3 kg	Elastic modulus, GPa	Porosity, %	Dry abrasion wear, mg/30 min
Conventional	A	0.16	1265 ± 211	281 ± 36	1.9 ± 0.37	8.5
	B	0.14	1088 ± 219	245 ± 21	2.04 ± 0.4	11.7
Sub-micron	A	0.33	1302 ± 124	244 ± 13	0.84 ± 0.17	10.7
	B	0.21	1147 ± 322	237 ± 27	0.7 ± 0.48	10.1

surface. In some areas, the whole material is worn (similar to cutting) and the porosity became smaller. On the other hand, in other areas abrasive particles interacted with the edges of pores and caused removal of material. The interaction of abrasive particles with the edge of pores leads to their widening. In addition, in images with 1000× magnification (Fig. 8c, d), removal of a group of carbides or splats is illustrated. However, higher magnification studies revealed additional wear mechanisms related to the interaction of abrasive particles with carbide grains. Figure 9(a) shows one spot after 3 h of wet abrasion testing and Fig. 9(b) shows exactly the same spot after 6 h of wet abrasion testing.

The following mechanisms that can happen step by step or simultaneously in the case of soft abrasive particles in wet abrasion test on WC-CoCr thermally sprayed materials are suggested:

1. Removal of soft metallic binder phase.
2. Fragmentation of carbide grains as a whole or in part.
3. Removal of fragments by removing the binder.

Larssen-basse et al. reported similar wear mechanism for soft abrasives (Ref 22). For a more detailed study, each carbide size shown in Fig. 9(a) was measured employing the image analysis software (Leica Qwin) and the above mechanisms were addressed by recourse to the relative size of the carbide grains to abrasive particles (average 220 nm). When this ratio is <0.5, cutting of binder and the removal of carbides with the binder occurs (Fig. 10a).

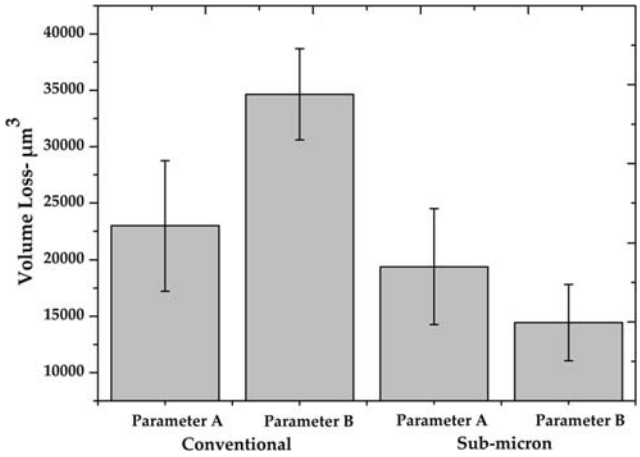

Fig. 6 Volume loss for conventional and sub-micron carbide size coatings in wet abrasion test sprayed with parameters A and B

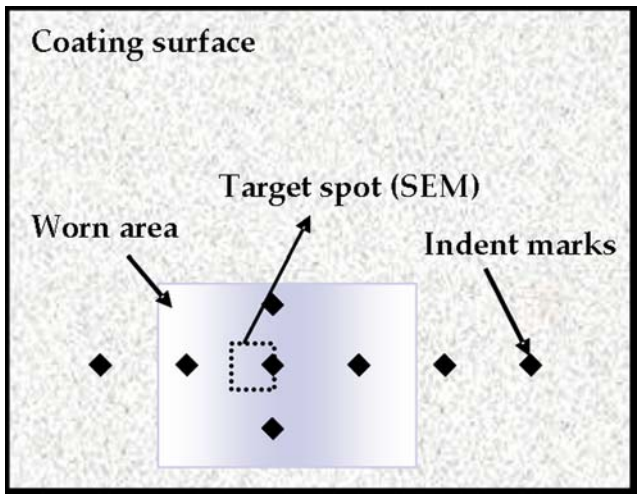

Fig. 7 Schematic of patterning and relocating procedure on the surface of WC-CoCr coating

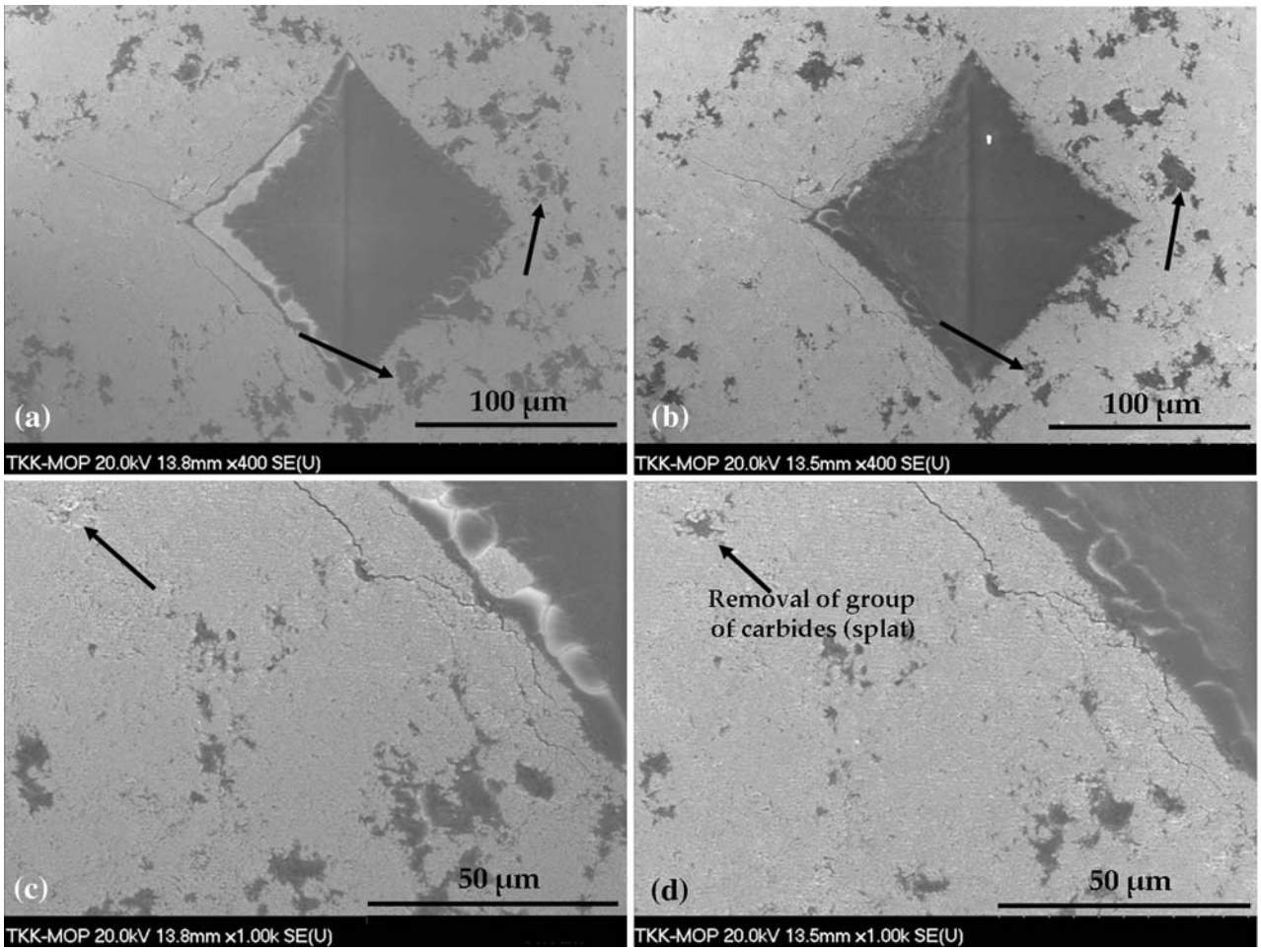

Fig. 8 After 3 h wet abrasion test 400× (a) and 1000× (c) and after 6 h test 400× (b) and 1000× (d)

When this ratio is between 0.7 and 1.3, fragmentation of carbides occurs. Note that when this ratio is close to the lower limit (0.7) fragmentation of whole grain happens and when it is close to higher limit (1.3) partial fragmentation of carbide grain occurs (Fig. 10b). With the ratio larger than 1.4, no significant effect on the carbides was

observed. All the above mechanisms were observed for spherical-like soft abrasive particles (in comparison to the coating material) in the wet abrasion test and might not be applicable for abrasives with different shape and different properties.

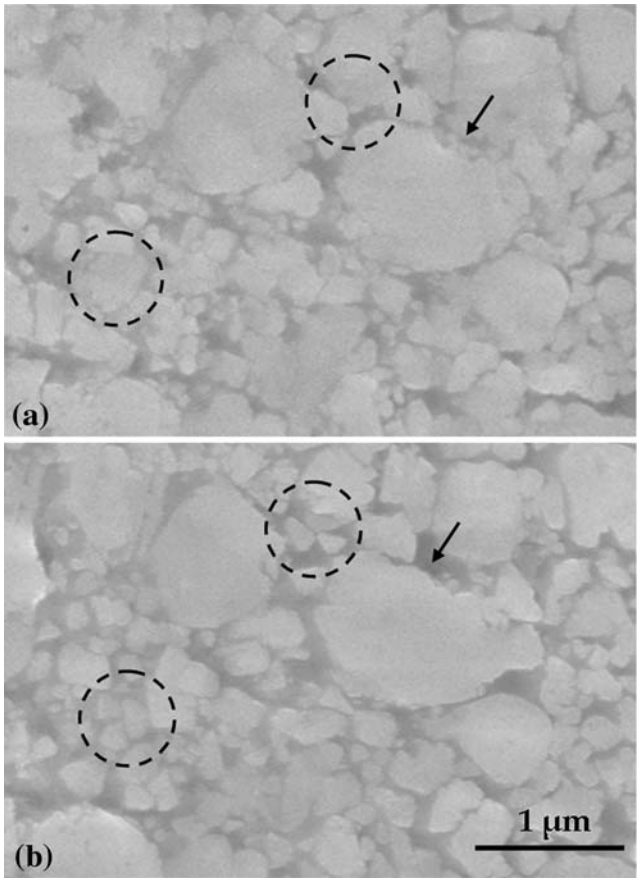

Fig. 9 High-magnification SEM images (a) taken after 3 h and (b) 6 h exposure to the wet abrasion test. Arrows indicate gradual removal of fragments and dotted circles indicate full or partial fragmentation of carbides

3.3 Wear Mechanism in Coarse Particle Dry Abrasion

Due to the formation of rough surfaces and high volume loss after dry sand abrasion test, study of the wear track in high magnification provides limited insight into underlying wear mechanism. One solution to overcome such limitations is studying the single scratches which have been made by individual abrasive particles in the very early stages of material removal. To be able to analyze the initial scratches and material removal caused by abrasive particles, sub-micron coatings sprayed with parameter ''B'' were exposed to the sand abrasion rubber wheel test for a very short time (one complete rotation of wheel at 30 rpm). The outcome of this test was a sample with single scratches on its surface. After the test, single scratches were studied by SEM.

When a rubber wheel (a cylinder) comes to the contact with a flat surface based on Hertzian theory (Ref 23), the contact pressure may have an elliptical distribution which has its maximum value in the center and the lowest values at its two ends. This contact pressure can be calculated as follows:

$$P(x) = P_{\max}\sqrt{1 - \frac{x^2}{a^2}} \quad \text{(Eq 1)}$$

$$a = \sqrt{\frac{4RF}{\pi E_R}} \quad \text{(Eq 2)}$$

$$P_{\max} = \frac{2F}{\pi a} \quad \text{(Eq 3)}$$

where $P(x)$, R, F, a, and E_R are pressure distribution, radius of rubber wheel, contact force per unit length of the cylinder during the test, half of contact length, and elastic modulus of rubber wheel, respectively.

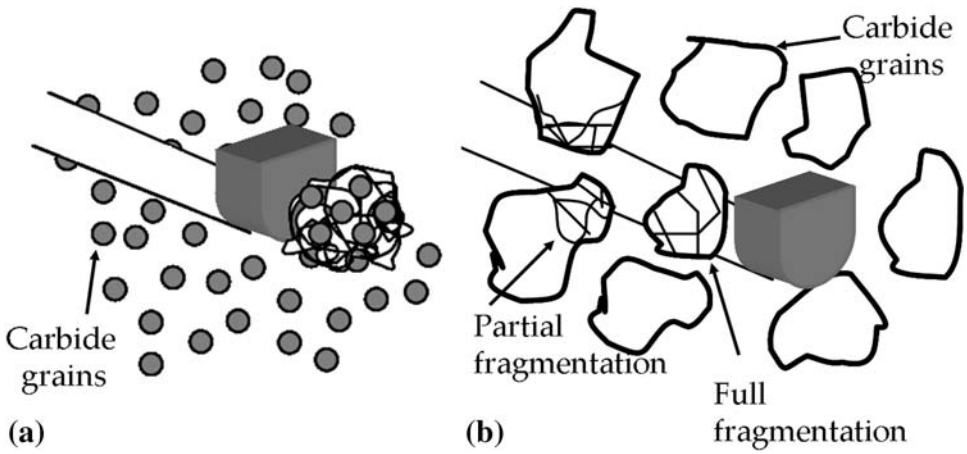

Fig. 10 Schematic of wear mechanisms: (a) removal of carbides by cutting the binder and (b) partial or full fragmentation of carbides

Figure 11(a) and (b) shows one example of the starting point of the scratches within the contact area and the continuance of same scratch, respectively. Similar to all other scratches, the scratches originated from surface open porosities and continued to the direction of rubber wheel movement. It is noteworthy that starting points of single scratches are not at the same pressure level in the contact region (based on pressure distribution of the rubber wheel in contact with rigid surface). This observation indicates that pressure level does not necessarily define the penetration point of abrasive particles into the material. The schematic of scratches formed on the surface within the contact region are shown in Fig. 11(c).

To remove material by abrasive particles, penetration of abrasives into the material and high enough shear force (parallel to the surface) acting on penetrated particle is necessary. In the case of relatively soft sand particles moving in between soft rubber wheel and hard coating surfaces, penetration of particles to the hard surface will be very limited. Nonetheless, in the current experiment, entrapment of the corner of an abrasive particle (which is sharp on the micro-scale) into the surface open porosities provides a condition similar to the already-penetrated particle. At this stage, a bigger portion of particle is gripped by rubber wheel and a smaller portion of particle is locked into the pore. Entrapment of a corner of an abrasive particle into the pore (similar to penetration of particle) and shear force provided by rotation of rubber wheel acting on abrasive particle satisfy two conditions for material removal by abrasive particles. Formation of grooves (Fig. 11b, c) with much smaller width than actual abrasive particle size (groove width 2-3 μm, abrasive particle size ~368 μm) provide evidence of the above explained mechanism which is based on entrapment of a corner of abrasive particle into the surface open porosities. The observed grooves are more likely microploughing and microcutting of material due to the single pass of an abrasive particle (Ref 24). In microploughing, the material does not detach from the surface and just displaces sideways. It can be displacing the hard WC within the soft binder. Microcutting can be cutting a shallow thickness of WC and cutting the binder which has been

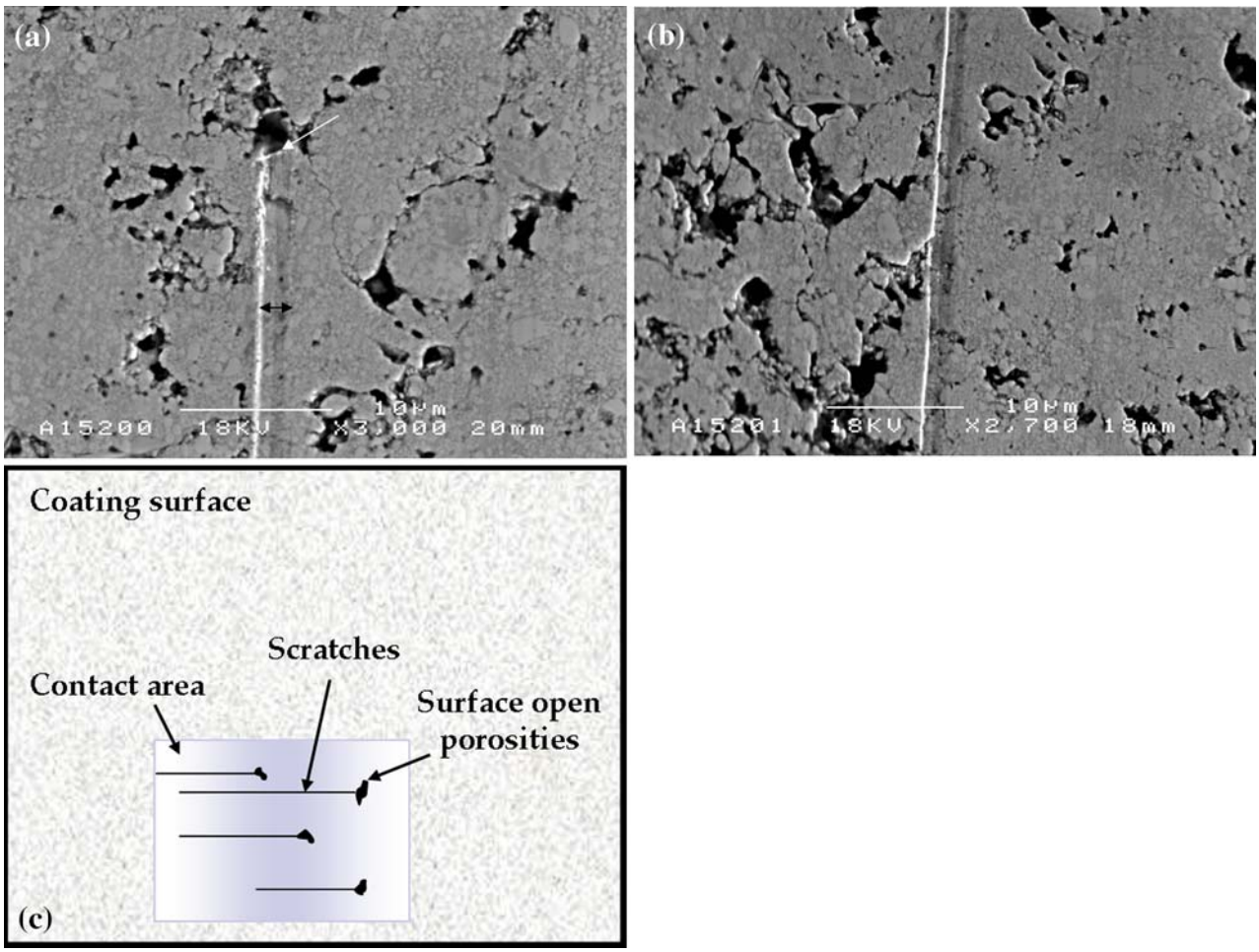

Fig. 11 (a) Starting point (shown by an arrow) of a single scratch from a surface open porosity and (b) middle part of scratch on the surface of coating in dry sand abrasion test. (c) Schematic of scratches formed on the surface within the contact region. Note that starting points are not related to the pressure distribution

extruded from between the WC grains. The microploughing was not pronounced to form significant ridges at the edges of grooves. This explanation is more plausible in the absence of debris and microcracking inside and around the wear grooves. In this experiment, microfatigue was not addressed as only one pass of single abrasive particle was considered and studied.

3.4 Effect of Surface Open Porosities on Wear Performance

When the surface open porosity size is smaller than the abrasive particle size, the pores will have a negative effect on wear performance as explained above (a corner of abrasive particle can be locked into the pore and start to scratch). Nonetheless, when the pore size is larger than the abrasive particle, the pore will act as a reservoir and abrasive particles will be deposited into that pore and the concentration of abrasive particles in contact with surface of material will be decreased. Consequently, the wear performance will be improved. It can be seen in Fig. 8(a) where the indent imprint acts as a big pore that abrasive particles can be deposited into the pore, resulting in less effected surface to the left side of indent mark (smooth with no pore produced by wear). Voyer and Marple observed the same positive effect of porosity on wear performance (Ref 25).

4. Conclusions

The behavior of WC-CoCr coatings produced with two different powders of varying WC grain size during wet and dry abrasion conditions was evaluated. W_2C/WC ratio was measured as a comparative tool to study the dissolution of WC into the matrix and its sensitivity to different variables. Dissolution of WC into the matrix is not sensitive to the spraying parameters for conventional powder. On the other hand, dissolution in sub-micron powder is more sensitive to spraying parameters. However, the hardness value was higher for higher W_2C content. No correlation between W_2C and wear performance in wet and dry abrasion test was observed. In addition, associated wear mechanisms under both wet and dry abrasion conditions were addressed. Reducing the carbide size from conventional to sub-micron did not lead to any significant gain in dry sand abrasion test. In fine particle wet abrasion test by reducing the carbide size from 1-3 μm to 0.4 μm the wear was reduced by 50%. Under wet abrasion condition where the abrasive medium contains titania particles mixed with water, the abrasive particles interact with binder and carbides separately. The wear mechanism consists of partial and/or full fragmentation of WC grains, removal of binder and removal of carbide fragments or small carbides within the binder. These steps can happen simultaneously or step-by-step. In the early stages of material removal, under dry abrasion condition, abrasive medium contains sand particles which are bigger than the carbides or binder mean free path. In this case, penetration of abrasive particle to the dense region of coating will be difficult. However, open surface pores will serve as origins for wear scratches made by individual abrasive particles. Intrinsic porosities which have been formed during the deposition process and can be found within the coatings have an effect on some of the mechanical properties such as elastic modulus, shear modulus, Poisson's ratio, and hardness that may indirectly affect the wear performance by changing the material's elastic-plastic response to the external loading. Dependency of mechanical properties on the porosity has been discussed extensively in literature (Ref 26-29). Nevertheless, when the porosities appear on the surface of a coating or are generated on the surface due to cutting or polishing process, the contact condition will be changed which causes the change in wear performance. To obtain the best wear-resistant carbide-based coatings, tailoring the carbide size will be more effective if we have adequate information on abrasive particle characteristics (size, hardness, and shape).

Acknowledgment

Arash Ghabchi gratefully acknowledges Professor Christopher Weyant from Center for Thermal Spray Research, Stony Brook University, for reviewing the manuscript and providing valuable comments.

References

1. J.R. Davis, *Handbook of Thermal Spray Technology*, Davis & Associates, ASM International, 2004
2. D. Chuanxian, H. Bingtain, and L. Huiling, Plasma-Sprayed Wear-Resistant Ceramic and Cermet Coating Materials, *Thin Solid Films*, 1984, **118**(4), p 485-493
3. J.M. Perry, A. Neville, and T. Hodgkiese, A Comparison of the Corrosion Behaviour of WC-CoCr, WC-Co HVOF Thermally Sprayed Coatings by In Situ Atomic Force Microscopy (AFM), *J. Therm. Spray Technol.*, 2002, **11**(4), p 536-541
4. D.A. Stewart, P.H. Shipway, and D.G. McCartney, Abrasive Wear Behaviour of Conventional and Nanocomposite HVOF-Sprayed WC-Co coatings, *Wear*, 1999, **225-229**, p 789-798
5. P.H. Shipway and J.J. Hogg, Dependence of Microscale Abrasion Mechanisms of WC-Co Hardmetals on Abrasive Type, *Wear*, 2005, **259**, p 44-51
6. Y. Qiao, Y. Liu, and T.E. Fischer, Sliding and Abrasive Wear Resistance of Thermal-Sprayed WC–Co Coatings, *J. Therm. Spray Technol.*, 2000, **10**(1), p 118-125
7. K. Jia and T.E. Fischer, Abrasion Resistance of Nanostructured and Conventional Cemented Carbides, *Wear*, 1996, **200**, p 206-214
8. C. Bartuli, T. Valente, F. Cipri, E. Bemporad, and M. Tului, Nanostructured WC-Co Coatings, *J. Therm. Spray Technol.*, 2005, **14**(2), p 187-195
9. A.H. Dent, S. DePalo, and S. Sampath, Examination of the Wear Properties of HVOF Sprayed Nanostructured and Conventional WC-Co Cermets with Different Binder Phase Contents, *J. Therm. Spray Technol.*, 2002, **11**(4), p 551-558
10. J.M. Guilemany, S. Dosta, J. Nin, and J.R. Miguel, Study of the Properties of WC-Co Nanostructured Coatings Sprayed by High-Velocity Oxyfuel, *J. Therm. Spray Technol.*, 2005, **14**(3), p 405-413
11. J.H. He and J.M. Schoenung, A Review on Nanostructured WC–Co Coatings, *Surf. Coat. Technol.*, 2002, **157**, p 72-79

12. B.R. Marple and R.S. Lima, Process Temperature/Velocity-Hardness-Wear Relationships for High-Velocity Oxyfuel-Sprayed Nanostructured and Conventional Cermet Coatings, *J. Therm. Spray Technol.*, 2005, **14**(1), p 67-76
13. Y.F. Qiao, T.E. Fischer, and A. Dent, The Effects of Fuel Chemistry and Feedstock Powder Structure on the Mechanical and Tribological Properties of HVOF Thermal-Sprayed WC–Co Coatings with Very Fine Structures, *Surf. Coat. Technol.*, 2003, **172**(1), p 24-41
14. P.H. Shipway, D.G. McCartney, and T. Sudaprasert, Sliding Wear Behavior of Conventional and Nanostructured HVOF Sprayed WC/Co Coatings, *Wear*, 2005, **259**, p 820-822
15. D.A. Stewart, P.H. Shipway, and D.G. McCartney, Microstructural Evolution in Thermally Sprayed WC–Co Coatings: Comparison between Nanocomposite and Conventional Starting Powders, *Acta Mater.*, 2000, **48**(7), p 1593-1604
16. Q.Q. Yang, T. Senda, and A. Ohmori, Effect of Carbide Grain Size on Microstructure and Sliding Wear Behavior of HVOF-Sprayed WC–12% Co Coatings, *Wear*, 2003, **254**(1-2), p 23-34
17. M. Watanabe, A. Owada, S. Kuroda, and Y. Gotoh, Effect of WC Size on Interface Fracture Toughness of WC–Co HVOF Sprayed Coatings, *Surf. Coat. Technol.*, 2006, **201**(3-4), p 619-627
18. J. He, Y. Liu, Y. Qiao, T.E. Fischer, and E.J. Lavernia, Near-Nanostructured WC-18 Pct Co Coatings with Low Amounts of Non-WC Carbide Phase: Part I. Synthesis and Characterization, *Metall. Mater. Trans. A*, 2002, **33**(1), p 145-157
19. ''Standard Test Method for Measuring Abrasion Using the Dry Sand/Rubber Wheel Apparatus,'' G65-94, *ASTM Standards*
20. ''Standard Test Method for Abrasive Wear Resistance of Cemented Carbides,'' B611-85, *ASTM Standards* (reapproved 1991)
21. C. Verdon, A. Karimi, and J.-L. Martin, A Study of High Velocity Oxy-Fuel Thermally Sprayed Tungsten Carbide Based Coatings. Part 1: Microstructures, *J. Mater. Sci. Eng. A*, 1998, **246**(1-2), p 11-24
22. J. Larsen-Basse and E.T. Koyanagi, Abrasion of WC-Co Alloys with Quartz, *J. Lubr. Technol. Trans.*, 1979, **101**(2), p 208-211
23. S.P. Timoshenko and J.N. Goodier, *Theory of Elasticity*, McGraw-Hill, New York, 1970
24. K.-H. Zum Gahr, Wear by Hard Particles, *Tribol. Int.*, 1998, **31**(10), p 587-596
25. J. Voyer and B.R. Marple, Sliding Wear Behavior of High Velocity Oxy-Fuel and High Power Plasma Spray-Processed Tungsten Carbide-Based Cermet Coatings, *Wear*, 1999, **225-229**(1), p 135-145
26. N. Ramakrishnan and V.S. Arunachalam, Effective Elastic Moduli of Porous Solids, *J. Mater. Sci.*, 1990, **25**(9), p 3930-3937
27. O. Hunter, Jr., and G.E. Graddy, Porosity Dependence of Elastic Properties of Polycrystalline Lu_2O_3, *J. Am. Ceram. Soc.*, 1976, **59**(1-2), p 82
28. M. Arnold, A.R. Boccaccini, and G. Ondracek, Prediction of the Poisson's Ratio of Porous Materials, *J. Mater. Sci.*, 1996, **31**(6), p 1643-1646
29. T. Nakamura, G. Qian, and C.C. Berndt, Effects of Pores on Mechanical Properties of Plasma Sprayed Ceramic Coatings, *J. Am. Ceram. Soc.*, 2000, **83**(3), p 578-584